Tip lengths and whiskering in noise-reduced diffusion-limited aggregation

1993 J. Phys. A: Math. Gen. 26 3431

(http://iopscience.iop.org/0305-4470/26/14/010)

J. Phys. A: Math. Gen. 26 (1993) 3431–3440. Printed in the UK

Tip lengths and whiskering in noise-reduced diffusion-limited aggregation

M T Batchelor† and B I Henry‡

† Mathematics Department, School of Mathematical Sciences, Australian National University, Canberra ACT 0200, Australia

‡ Department of Applied Mathematics, University of New South Wales, Kensington NSW 2033, Australia

Received 8 October 1992, in final form 12 March 1993

Abstract. We examine the nature of the tunable family of patterns obtained from the discrete η-DLA model in the deterministic zero-noise limit. The η-DLA model is a variant of the standard diffusion-limited aggregation (DLA) model in which the DLA growth probabilities are raised to the power η. The observed morphologies, which range from compact Eden clusters for $\eta = 0$ through to sharp needle-like clusters with increasing η, can be characterized by a sequence of step lengths in a stable staircase structure proceeding back from the tip. Side-branch whiskers, which are found on the triangular lattice but not on the square lattice, occur closer to the tip as η is increased. Beyond a value η_c, whiskers are found immediately behind the tip.

We derive the length of the exposed tip as a function of η using a stationary contour approximation and conformal mapping methods. A theoretical estimate for η_c is derived by refining this approach to incorporate the possible shielding of surface sites by aggregate sites. Our theoretical results are in excellent agreement with the numerical results on both lattices.

1. Introduction

The Witten–Sander diffusion-limited aggregation (DLA) model [1] and its variants have been widely studied as paradigms for the growth of fractal structures [2] (for reviews, see e.g. [3–5]). Despite intensive effort however, the DLA model remains a major theoretical challenge. In this model, and the related dielectric breakdown (DB) model [6], particles are added one at a time to a growing cluster by choosing a single surface site at random according to a Laplacian probability distribution. In simpler models, such as the Eden [7] and Williams–Bjerknes [8] models, the growth site probability distribution is essentially uniform, resulting in compact growth.

Particularly interesting variants of these models exhibiting a tunable range of patterns, from compact to fractal, are the η-DLA [9] and η-DB [6] models. In these models the surface site growth probabilities are raised to a power η prior to each growth step. When $\eta = 0$ the η-DLA model reduces to the Eden model whereas the η-DB model reduces to the Williams–Bjerknes model.

A second parameter that can be introduced into the models is a noise reduction parameter m [10–12], whereby a potential growth site must be selected m times before growth occurs. The effect of increasing m is to average out the growth instabilities and in the limit $m \to \infty$ the growth is fully deterministic. Studies of the noise-reduced variants have led to significant theoretical progress in understanding the role of fluctuations in the growth and form of the Laplacian models [13, 14].

0305-4470/93/143431+10$07.50

In a recent series of papers we have examined the deterministic zero-noise limit for a variety of non-equilibrium growth models. These include the Eden [15], DLA and DB [16, 17] models on the square and cubic lattices, and generalized DLA models on the square [18] and triangular [19] lattices. For zero-noise DLA in the absence of surface tension, growth is in the form of a stable needle-star with the tips directed along the lattice axes. The star arms are characterized by a needle staircase with constant step lengths independent of the aggregate size. The needle-star aggregates are compact on the square lattice [12, 13, 16, 17, 20] but regular side branches (whiskers) develop back from the tips on the triangular lattice [19] (see figure 1 where a tip of the needle-star is exhibited for each lattice).

Random fractal structures are observed in the zero-noise limit on random lattices [21].

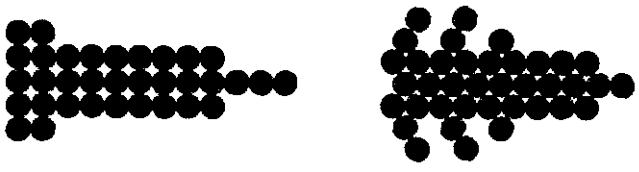

Figure 1. Illustration of the stable tip shapes of regular DLA ($\eta = 1$) on the (a) square and (b) *triangular lattices. In each case the tip propagates to the right.*

The nature of growth in the zero-noise limit provides a clear indication of the relevance of fluctuations in fractal pattern formation. The limit also provides an ideal testbed for the stationary contour approximation and conformal mapping approach [13, 14] which we have developed to provide a theoretical understanding of stable needle staircases and tip-splitting as a function of increasing surface tension [18, 19]. However, whilst our theoretical analysis (which should be thought of as a lowest-order approximation) was successful in describing detailed features of the staircase structures and of tip-splitting it did not explain the whiskering that we had observed in numerical simulations of DLA on the triangular lattice.

In this paper we present numerical and theoretical results for the zero-noise limit of the η-DLA model on the square and triangular lattices. In numerical simulations, we explore the full range of pattern formation from compact Eden growth at $\eta = 0$ to regular DLA needle-star growth at $\eta = 1$ to elongated needle-stars for $\eta > 1$. The range $\eta > 1$ is of additional interest as we observe whiskering in the first step above the tip on the triangular lattice for $\eta > \eta_c > 1$. Theoretical estimates for the length of the exposed stable tip as a function of η are derived from the stationary contour approximation and conformal mapping methods. A theoretical estimate for the value η_c, for whiskering in the first step, is then derived by refining this approach to include nearest-neighbour screening effects.

2. Numerical results

The surface growth probabilities in the η-DLA model [9] are defined by

$$p = \left[\frac{1}{q}\sum_{\text{nn}}\phi\right]^{\eta} \tag{1}$$

where q is the lattice coordination number, ϕ is a field variable and the sum is over all nearest neighbours. The field variable ϕ is defined by the discrete Laplace equation

$$\phi = \frac{1}{q}\sum_{\text{nn}}\phi \tag{2}$$

together with the boundary conditions

$$\phi = \begin{cases} 1 & \text{distant boundary} \\ 0 & \text{aggregate and surface sites.} \end{cases}$$

In the zero-noise limit particles are added to the growing cluster in layers by converting the most probable surface sites to aggregate sites at each level of growth. Those surface sites that are not fully converted to aggregate sites are partially converted in proportion to their growth probabilities. This partial conversion is then accounted for when considering growth at the next level. The growth algorithm can be readily implemented as follows: at a given level l we define a set of weights $w^{(l)}$ by

$$w^{(l)} = (1 - r^{(l-1)})/p^{(l)} \tag{3}$$

where $r^{(l-1)}$ are accumulated residues from the previous level and $p^{(l)}$ are the normalized *a priori* growth probabilities. Each level of growth corresponds to the conversion of the set of minimum weight surface sites into aggregate sites. The set of surface sites that are not converted to aggregate sites accrue a further residue $pw_{\min}$, i.e.

$$r^{(l)} = p^{(l)}w^{(l)}_{\min} + r^{(l-1)}. \tag{4}$$

Details of our numerical scheme for obtaining zero-noise Laplacian growth have been reported elsewhere [16, 18, 19] (see also [20–24]).

2.1. Square lattice

Numerical results for zero-noise η-DLA cluster morphologies as a function of η are summarized in figure 2 (square lattice) and figure 3 (triangular lattice). On the square lattice, the cluster has a diamond-shaped envelope for $\eta \simeq 0$, as anticipated by the correspondence with the Eden model at $\eta = 0$. Note the presence of fjords at the centre of the faces of the diamonds for $\eta = 0.1$. These fjords do not appear for $\eta = 0$ or for $\eta < 0$. As η is increased above zero the fjords widen and the cluster evolves into a petal-shaped star with the star tips directed along the lattice axes. The tips of the star are characterized by a stable staircase structure. In the η-DLA model the staircase structure persists down to the Eden limit $\eta = 0$ where all steps have length one. As η is increased further the step lengths in the staircase increase and the star tips become more needle-like. For example, the tip length is three or four units at $\eta = 1$ (regular DLA).

2.2. Triangular lattice

The cluster morphology as a function of η exhibits a similar pattern on the triangular lattice with two essential differences:

(i) the limit $\eta = 0$ yields a hexagonal-shaped cluster having a staircase structure with step lengths of one-half (consistent with zero-noise Eden growth on the triangular lattice); and

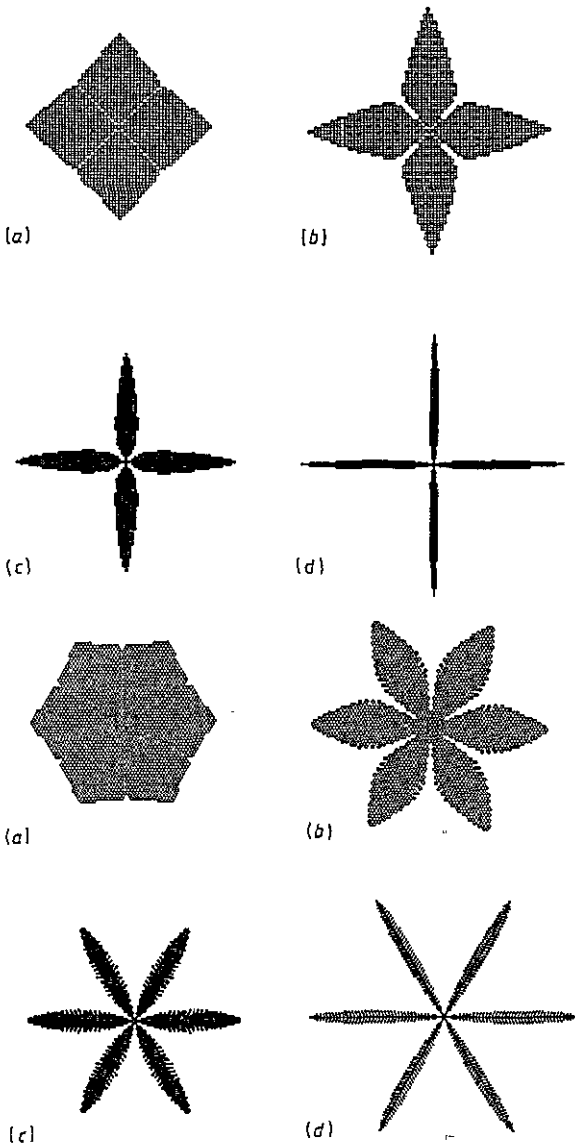

Figure 2. Initial levels of growth in the zero-noise limit of η-DLA on the square lattice. The parameters are: (*a*) $\eta = 0.1$, $N = 1489$; (*b*) $\eta = 0.5$, $N = 1453$; (*c*) $\eta = 0.8$, $N = 1401$; (*d*) $\eta = 1.2$, $N = 1281$. The limit $\eta = 0$ is a perfect diamond.

Figure 3. Initial levels of growth in the zero-noise limit of η-DLA on the triangular lattice. The parameters are: (*a*) $\eta = 0.1$, $N = 2233$; (*b*) $\eta = 0.5$, $N = 2185$; (*c*) $\eta = 0.8$, $N = 2107$; (*d*) $\eta = 1.2$, $N = 1909$. The limit $\eta = 0$ is a perfect hexagon.

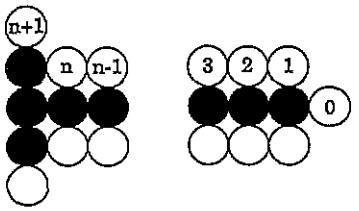

Figure 4. Labelling of surface growth probabilities for the square lattice.

(ii) the needle stars exhibit whiskering back from the tips.

The whiskering is of particular interest because it clearly demonstrates branching (a precursor to fractal pattern formation) without noise in on-lattice Laplacian growth. This

whiskering is also apparent in zero-noise regular DLA ($\eta = 1$) on the triangular lattice [19] †. In the generalized η-DLA model we have a relevant parameter η to focus theoretical studies of the whiskering. For example, at $\eta = 1$ the whiskering occurs in the second step above the tip whereas for $\eta > \eta_c > 1$ whiskering occurs in the first step above the tip. The tip length at $\eta = 1$ (regular DLA) is 1.5 or 2.5 units.

3. Theoretical results

The development of a petal-star-shaped cluster from the regular Eden cluster as η is increased above zero can be readily explained. Introducing a finite η value changes the growth from Eden to Laplacian. In Eden growth the growth probabilities are uniform on all surface sites of the cluster whereas in Laplacian growth the growth probabilities are uniform at all points on a circle centred on and containing the cluster. The growth probabilities are highest at surface sites closest to this circle and lowest at surface sites furthest from this circle. Thus introducing a finite η value increases the probability for growth at the vertices of the initial diamond (square lattice) or hexagon (triangular lattice) and decreases the probability for growth along the faces, with minimum probability for growth at the centres of these faces. This then has the effect of producing fjords at the centres of the faces and branching along the direction of the vertices.

In earlier work we derived details of the branch tips by employing a stationary contour approximation to obtain expressions relating the step lengths in the stable needle staircases to the surface growth probabilities [18, 19].

3.1. Square lattice

On the square lattice we label the surface growth probabilities back from the tip by $p_0, p_1, p_2, \ldots$ as in figure 4. The condition for growth at site $n+1$ (rather than at the tip) is then given by [18]

$$\sum_{j=1}^{n} p_j < p_0 < \sum_{j=1}^{n+1} p_j \tag{5}$$

and the length of the tip is $l_1 = n$ or $n+1$. The surface growth probabilities in (5) can be evaluated by combining a stationary contour approximation with conformal mapping methods. In this approach [13] the growth probability at a surface site around a tip is approximated by the probability for an off-lattice walker to contact an interval $[P_j, P_{j+1}]$ on a stationary contour. The latter probabilities are calculated by conformally mapping the stationary contour onto a circle or a straight line—the probabilities are proportional to the length of the transformed interval $|P'_j - P'_{j+1}|$ under the conformal mapping. In the η-model these probabilities are then raised to the power η.

On the square lattice we consider probabilities derived from the conformal mapping of a protrusion with: (i) a semi-circular tip and (ii) a square tip onto a straight line. The transformation [13]

$$w = \frac{\pi}{2} z^2 + z\sqrt{z^2+1} + \ln\left(z + \sqrt{z^2+1}\right) \tag{6}$$

† In contrast, at $\eta = 1$ the DB model exhibits tip-splitting into eight major arms on the square lattice [16, 18, 20] and twelve major arms on the triangular lattice [19]. Similarly the regular DB model exhibits tip-splitting on the cubic lattice, whereas regular DLA has six stable arms [16, 17].

maps the exterior of a protrusion with width $2a$ and an essentially semi-circular tip to the right half-plane, with the contour going to the imaginary axis. Here the lattice spacing $a = \pi/2$. The transformation [18]

$$w = \frac{2a}{\pi}\left[\ln\left(z + \sqrt{z^2-1}\right) - z\sqrt{z^2-1}\right] - \mathrm{i}a \tag{7}$$

maps the exterior of a protrusion with width $2a$ and a square tip to the upper half-plane, with the contour going to the real axis.

The surface growth probabilities are now calculated from

$$p_0 = |2P_1'|^\eta \quad p_j = |P_{j+1}' - P_j'|^\eta \qquad j = 1, 2, \ldots \tag{8}$$

where the P' are obtained by conformally mapping the points

$$P_j = \left(-\frac{2j-1}{2}a, a\right) \qquad j = 2, 3, \ldots \tag{9}$$

and

$$P_1 = \begin{cases} (-a\cos^2\theta, a\sin^2\theta) & \text{semi-circular tip} \\ (0, a) & \text{square tip.} \end{cases} \tag{10}$$

In the above, $\theta \simeq 0.96939$. Tip lengths in the η-DLA model on the square lattice can now be readily calculated from (5) by calculating p_j as outlined above. Our theoretical results, together with our numerical measurements, are listed in table 1. There is excellent agreement over the full range of η for which numerical measurements were made.

Table 1. Theoretical estimates for the length ℓ_1 of the exposed tip in η-DLA as a function of η on the square lattice for the indicated contours. The exact numerical values are shown for comparison.

ℓ_1	Semi-circular	Square	Numerical
1–2	$\eta < 0.72$	$\eta < 0.65$	$\eta < 0.59$
2–3	$0.73 < \eta < 0.97$	$0.66 < \eta < 0.88$	$0.60 < \eta < 0.86$
3–4	$0.98 < \eta < 1.11$	$0.89 < \eta < 1.02$	$0.87 < \eta < 1.03$
4–5	$1.12 < \eta < 1.21$	$1.03 < \eta < 1.11$	$1.04 < \eta < 1.14$
5–6	$1.22 < \eta < 1.28$	$1.12 < \eta < 1.18$	$1.15 < \eta < 1.22$
6–7	$1.29 < \eta < 1.33$	$1.19 < \eta < 1.23$	$1.23 < \eta < 1.29$

3.2. Triangular lattice

As mentioned previously our theoretical approach has been less satisfactory in accounting for detailed features in DLA growth on the triangular lattice. In a lowest-order treatment we can proceed as for the square lattice [18]. To take into account the staggered nature of alternate layers of growth, we label the surface growth probabilities as in figure 5, and derive the condition for growth at site $n + \frac{1}{2}$ ahead of further growth at the tip [19],

$$\sum_{j=1}^{n} p_{2j-1} < p_0 < \sum_{j=1}^{n+1} p_{2j-1}. \tag{11}$$

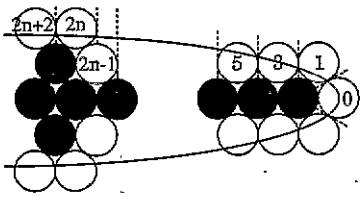

Figure 5. Labelling of surface growth probabilities for the triangular lattice. Note that the surface (open circles) at site $2n-1$ is shielded by the surface at site $2n$. The reduced contour interval due to this shielding is also shown.

This condition defines the length of the exposed tip as $l_1 = n - \frac{1}{2}$ or $n + \frac{1}{2}$. On the triangular lattice a good approximation to the surface growth probabilities can be obtained from the conformal mapping of a six-armed star with a well defined exterior but no width. The probability for growth along an interval $[P_a, P_b]$ of the arm is given by

$$p_a = \int_{P_b}^{P_a} \frac{6}{\pi} \frac{y^2}{(1-y^6)^{1/2}} \, dy \tag{12}$$

It is a simple matter to assign intervals to surface sites on the triangular lattice and then to evaluate the integral in (12) and thus derive the surface growth probabilities. The results are (see also [19])

$$\begin{aligned} p_k &= \frac{2}{\pi}[\sin^{-1}(P_k^3) - \sin^{-1}(P_{k+2}^3)] \qquad k \geqslant 1 \\ p_0 &= 2[1 - \frac{2}{\pi}\sin^{-1}(P_1^3)] \end{aligned} \tag{13}$$

where

$$\begin{aligned} P_k &= 1 - c_k/L \\ c_k &= (k-1)/2 \qquad k > 1 \end{aligned} \tag{14}$$

and the remaining c_1 is defined by the local geometry of the tip. In the results reported here we have considered a triangular tip ($c_1 = .25$) and a parabolic tip ($c_1 \simeq 0.2087$). To calculate tip lengths in the η-DLA model on the triangular lattice we make the replacement, $p_i \to p_i^\eta$, in (11). Results from this analysis are compared with numerical results in table 2. Excellent agreement is obtained for the triangular contour in the range $\eta < 1.1$†. However, for η greater than this critical value, the numerical simulations provide evidence of whiskering with the tip length alternating between *three* distinct values. By contrast, the above theoretical analysis always predicts a tip length alternating between *two* different values.

Table 2. Theoretical estimates for the length ℓ_1 of the exposed tip in η-DLA as a function of η on the triangular lattice for the indicated contours. The estimates for the three-step values follow from equations (16) and (17) where screening of surface sites is taken into account. The exact numerical values are shown for comparison.

ℓ_1	Triangular	Parabolic	Numerical
0.5–1.5	$\eta < 0.88$	$\eta < 1.07$	$\eta < 0.84$
1.5–2.5	$0.89 < \eta < 1.23$	$1.08 < \eta < 1.45$	$0.85 < \eta < 1.10$
1.5–2.5–3.5	$0.93 < \eta < 1.23$	$1.08 < \eta < 1.45$	$1.11 < \eta < 1.56$
2.5–3.5–4.5	$1.24 < \eta < 1.43$	$1.46 < \eta < 1.65$	$1.57 < \eta < 1.8$

† Note that the approach of [14] approximating the outer envelope of the tip as a wedge predicts an envelope head angle at $\eta = 1$ of (i) $\theta_G = 164.0°$ for the square and (ii) $\theta_G = 155.8°$ for the triangular lattices. These results are in excellent agreement with the observed values in the zero-noise limit: (i) $\theta_G = 162°$ or $166°$ and (ii) $\theta_G = 150°$ or $160°$. It would be most interesting to extend these results away from $\eta = 1$.

3.3. Whiskering

Whiskering on the triangular lattice arises from shielding whereby the outermost surface site on one step of a staircase partially shields the innermost surface site on the step of the staircase that is one level down (see figure 5). It is a simple matter to compute growth probabilities that take this shielding into account using the stationary contour approximation. The contour intervals associated with the growth at a shielded site are reduced by a factor two (see figure 5) and hence the shielded growth probabilities, p^* are given by

$$p_k^* = \frac{2}{\pi}[\sin^{-1}(P_k^3) - \sin^{-1}(P_{k+1}^3)]. \tag{15}$$

One immediate consequence of this is that growth may be favoured at site $2n-1$ over further growth at the tip when $2n-1$ is unshielded whereas growth may be favoured at the tip if $2n-1$ is shielded. Consider such a situation for a row of particles with a surface at site $2n$ shielding a surface at site $2n-1$—this may correspond to the first step in a needle staircase with tip length $n-\frac{1}{2}$ (figure 6(*a*)). Due to the shielding next growth would then occur at the tip increasing the tip length to $n+\frac{1}{2}$ (figure 6(*b*)). The surface at site $2n$ is thus shifted back to site $2n+2$, the shielded surface is shifted back to site $2n+1$ and we now have an unshielded surface at site $2n-1$. Hence growth at site $2n-1$ is now preferred over growth at the tip and this produces a surface gap at site $2n+1$—the particle at site $2n-1$ is a whisker (figure 6(*c*)). The tip length is now $n-\frac{3}{2}$.

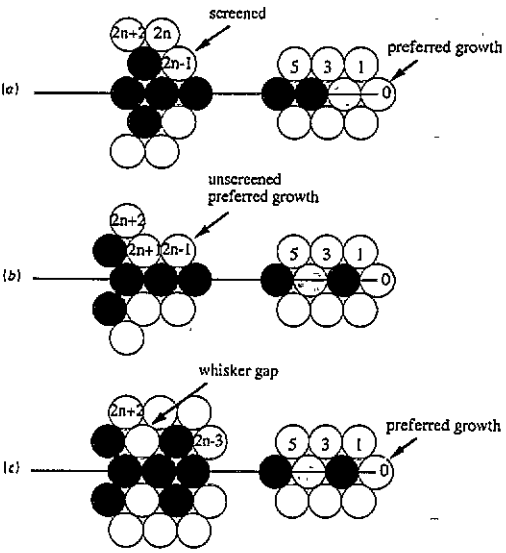

Figure 6. Steps in the formation of a whisker at site $2n-1$ with a first step length alternating between (*a*) $n-\frac{1}{2}$, (*b*) $n+\frac{1}{2}$ and (*c*) $n-\frac{3}{2}$. Open circles denote surface sites.

We have used the above scenario to motivate a derivation of conditions for whiskering with a tip length alternating between three values. Explicitly we find that whiskering with a tip length of 1.5, 2.5, 3.5 can occur provided that

$$\begin{aligned} &p_1 + p_3 < p_0 < p_1 + p_3 + p_5 \\ &(p_0 - p_1 - p_3)(p_3 - p_3^* + p_7^*) < (p_0 - p_1 - p_3^* - p_5^*)p_5. \end{aligned} \tag{16}$$

Similarly we find that whiskering with a tip length of 2.5, 3.5, 4.5 can occur provided

$$\begin{aligned} &p_1 + p_3 + p_5 < p_0 < p_1 + p_3 + p_5 + p_7 \\ &(p_0 - p_1 - p_3 - p_5)(p_5 - p_5^* + p_9^*) < (p_0 - p_1 - p_3^* - p_5^* - p_7^*)p_7. \end{aligned} \tag{17}$$

The inequalities, (16) and (17) define a range of η values for whiskers with tip lengths 1.5, 2.5, 3.5 and 2.5, 3.5, 4.5 respectively. Results from this theoretical analysis are compared with results from numerical simulations in table 2. There is good agreement between the theoretical and numerical values, particularly for the parabolic contour, which predicts a value $\eta_c \simeq 1.08$ (numerical $\eta_c \simeq 1.11$) for the first appearance of the three-step with whiskers directly behind the tip.

4. Conclusion

On-lattice simulations of the η-DLA model were compared with theory in the deterministic zero-noise limit. The observed morphologies were found to range from compact Eden clusters for $\eta = 0$ through to needle-star clusters with increasing η. Conformal mapping methods together with a stationary contour approximation were employed to estimate the tip length as a function of η and excellent agreement was obtained with the numerical simulations. On the triangular lattice, but not the square lattice, side-branch whiskers were observed which occur closer to the tip as η is increased. We were able to account for the whiskering by including an effective shielding in the stationary contour approximation. The shielding is due to the staggered nature of growth on the triangular lattice. On the square lattice where growth layers stack directly on top of each other there is no analogous shielding.

Acknowledgments

MTB has been supported by the Australian Research Council. The calculations reported here were carried out on the Fujitsu VP-2200 at the Australian National University Supercomputer Facility.

References

[1] Witten T A and Sander L M 1981 *Phys. Rev. Lett.* **47** 1400
[2] Mandelbrot B B 1982 *The Fractal Geometry of Nature* (San Francisco: Freeman)
[3] Meakin P 1988 in *Phase Transitions and Critical Phenomena* vol 12, ed C Domb and J Lebowitz (New York: Academic) p 135
[4] Vicsek T 1989 *Fractal Growth Phenomena* (Singapore: World Scientific)
[5] Matsushita M 1989 *The Fractal Approach to Heterogeneous Chemistry* ed D Avnir (Chichester: Wiley) p 161
[6] Niemeyer L, Pietronero L and Wiesmann H J 1984 *Phys. Rev. Lett.* **52** 1033
[7] Eden M 1961 *Proc. 4th Berkley Symp. on Mathematical Statistics and Probability* vol 4, ed F Neyman (Berkley, CA: University of California Press) p 223
[8] Williams T and Bjerknes R 1972 *Nature* **236** 19
[9] Nittmann J and Stanley H E 1987 *J. Phys. A: Math. Gen.* **20** L1185
[10] Tang C 1985 *Phys. Rev.* A **31** 1977
[11] Nittmann J and Stanley H E 1986 *Nature* **321** 663
[12] Kertész J and Vicsek T 1986 *J. Phys. A: Math. Gen.* **19** L257
[13] Eckmann J-P, Meakin P, Procaccia I and Zeitak R 1989 *Phys. Rev.* A **39** 3185

[14] Bali R C, Barker P W and Blumenfeld R 1991 *Europhys. Lett.* **16** 47
[15] Batchelor M T and Henry B I 1991 *Phys. Lett.* **157A** 229
[16] Batchelor M T and Henry B I 1992 *Phys. Rev.* A **45** 4180
[17] Batchelor M T and Henry B I 1992 *Physica* A **191** 113
[18] Batchelor M T and Henry B I 1992 *Physica* A **187** 551
[19] Batchelor M T, Dun C R and Henry B I 1993 *Physica* **193A** 553
[20] Moukarzel C 1992 *Physica* A **188** 469
[21] Moukarzel C 1992 *Physica* A **190** 13
[22] Garik P, Richter R, Hautman J and Ramanlal P 1985 *Phys. Rev.* A **32** 3156
[23] Garik P, Mullen K and Richter R 1987 *Phys. Rev.* A **35** 3046
[24] Herrmann H J, Kertész J and de Arcangelis L 1989 *Europhys. Lett.* **10** 147